Journal of
Ship&Ocean
Technology
©SEPTEMBER 2002

SOTECH Vol. 6, No. 3, pp. 1~12, 2002

Experimental Investigations on the Plastic Damage of Plates due to Lateral Collisions

Sang-Rai Cho[1], Il-Woong Kim[2] and Sang-Bock Lee[3]

[1]School of Transportation Systems Engineering, University of Ulsan, Nam-Ulsan P.O. Box 18, Ulsan, 680-749, Korea; E-mail: srcho@uou.ulsan.ac.kr
[2]University of Ulsan, presently Hyundai Heavy Industries
[3]University of Ulsan, presently STX Shipbuilding Industries

Abstract

In this paper the results are reported of sixty-nine lateral collision tests, which were performed to investigate the collision resistance of plates. For the tests a collision testing machine of spring-roller conveyer type was designed and fabricated. Using this machine, various plates were tested with different masses and velocities and various headers of the striker.
A simple analytical method has also been developed to predict the extent of damage of struck plates due to lateral collision. In the method, it is assumed that the kinetic energy of the striker can be dissipated by the formation of yield lines and membrane tensions in the impacted plate. The calculated predictions of extent of damage using the developed method have been substantiated with the test results, which shows reasonably acceptable correlations.
Keywords: plate, lateral collision test, simple analytical method, extent of damage

Notation

E	Young's modulus of the material
E_k	kinetic energy of the striker
E_p	energy absorption capacity of the plate
M	mass of the striker
U_b	plastic strain energy dissipated by formation of yield lines
U_t	plastic strain energy dissipated by membrane tension
U_{total}	total strain energy dissipated by the impacted plate, $U_b + U_t$
V_i	impact velocity of the striker
a	height of the plate
b	width of the plate
m_p	fully plastic bending moment of plate of unit length, $\sigma_{YD}t^2/4$
t	thickness of the plate

δ	depth of dent of struck plate
$\dot{\varepsilon}$	strain rate of the material
ε_r	rupture strain of the material
σ_Y	static yield stress of the material
σ_{YD}	dynamic yield stress of the material
σ_{ult}	tensile stress of the material

1 Introduction

Recently ship collision is more probable than before because ships are becoming larger and faster, especially those of tankers, container ships and passenger ships. Collision accidents may cause economic losses and sea pollution and sometimes even human life losses. Generally deformations of ship structures due to collision occur in a very short period remaining large permanent deformation and rupture. Therefore it requests dynamic nonlinear structural analyses. However, by the aids of supercomputers, detailed collision analyses are now able to be performed using commercial computer codes. But the analysis results using those codes have not yet been fully substantiated with the results of experimental investigations and the economic aspect of using these commercial packages for impacted ship structure analyses has not been justified yet(Kitamura and Kuroiwa 1996).

In order to cope with the accidents like ship collisions in more rational way, it is firstly necessary to quantify the possibility of the occurrence of accidents. Secondly we need to predict the probable extent of damage due to the prescribed scenarios of the accidents and then the residual strength of the damaged structures(Frieze and Cho 1989). Having tools to follow the above mentioned analysis procedures the lifetime cost optimization can be performed and which can provide the structural design guidance against collision accidents. However, it seems not still possible to employ any practical tools to trace the procedures in structural design stage.

Even though plate is a basic structural element of marine structures only few tests subjected to lateral collision loads were reported(Samuelides 1984, Zhu and Faulkner 1993). In this paper, the results of sixty-nine lateral collision tests on plates are reported aiming to provide experimental information on the lateral collision responses of plate. Before the collision tests, the material properties of the models were quantified through static and dynamic tensile tests. Collision tests were then performed changing the velocity and mass of the striker and the striker header type. The collision testing machine used is of spring/roller conveyer type, where free rebound is allowed as in the real situation. The deformed shapes of the damaged models were measured afterwards.

In this study an analytical method is also proposed to predict the extent of damage of plates subjected to lateral collision. In the method, the kinetic energy of the striker is assumed to be dissipated by the formation of yield lines and plastic membrane tensions in the impacted plate. The calculated predictions using this theoretical method have been substantiated with the collision test results.

The test results provided in this paper are expected to be useful to substantiate any predictions by theoretical methods or design formulations. The proposed analytical method can be extended and possibly applied to more complicated structures.

2 Lateral collision tests

2.1 Collision testing machine

The collision testing machine used in this study is consist of a striker, an accelerator, a roller conveyer, a model supporter and two velocity measurement devices, which can be seen in Figure 1. Three types of striker header were used namely, those of knife edge, square and rectangular. The accelerator consists of four steel bars and springs, which were designed to convert the strain energy of the compressed springs into the kinetic energy of the striker. The velocity of the striker can be controlled by changing the compressed length of the springs. The velocity of the striker can be increased up to $8m/sec.$ and the mass can vary between 20-60kg. The accelerated striker runs on the roller conveyer, which minimizes the friction as low as possible.

Two types of velocity measurement systems are equipped as shown in Figure 1. One consists of a timer and two light sensors. The first light sensor starts the timer and the other stops it. The impact velocity of the striker is calculated dividing the distance between two sensors by the measured time duration. The other velocity measurement system consists of an one-chip micro processor and four light sensors with which not only the Impact velocity but also the rebound velocity can be obtained.

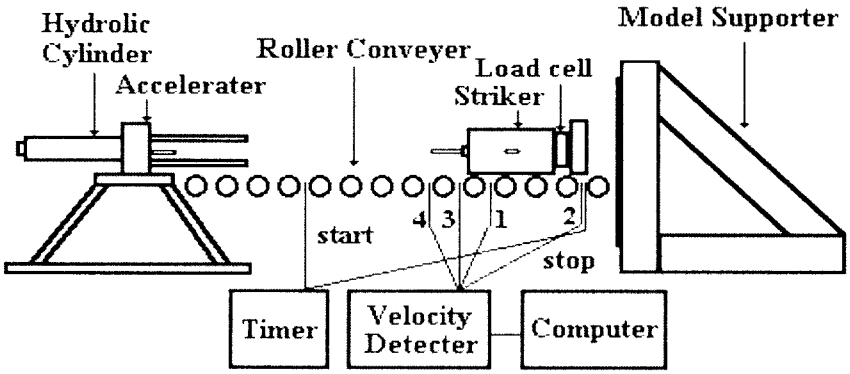

Figure 1: Sketch of the collision testing machine together with velocity measurement systems

2.2 Test models and tensile tests

For the collision tests, sixty-nine models were prepared of mild steel. The testing size of thirty-nine models was of $500mm \times 300mm$(the actual size was of $700mm \times 500mm$), that of twenty-four models was of $700mm \times 500mm$(the actual size was of $900mm \times 700mm$) and that of the other six models was of $770mm \times 500mm$(the actual size was of $970mm \times 700mm$). In the tests the models were firmly fixed to the model supporter by bolting. The geometry and material properties of the models are summarized in Table 1.

In order to obtain the mechanical properties of test model materials static and dynamic tensile tests were carried out. For the tensile tests the specimens were machined according to the Korean standard regulations. From the static tensile tests the static yield stress and Young's modulus were obtained and average values of them are shown in Table 1. For the models of D and E series,

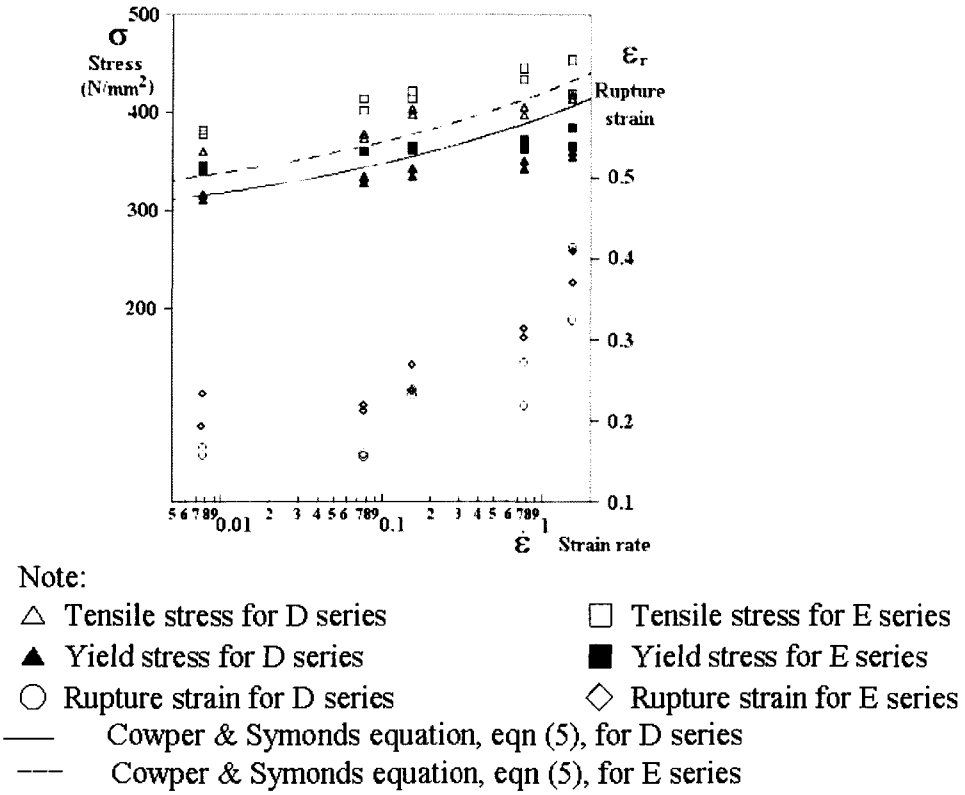

Figure 2: Effects of strain rate on the yield stress, tensile stress and rupture strain of mild steel plates

dynamic tensile tests were also performed and the yield stress, the tensile stress and the rupture strain for different strain rates were obtained. The effects of strain rate on the yield stress, the tensile stress and the rupture strain of the material are illustrated in Figure 2. As can be seen in the figure when increasing the strain rate all of the three quantities can be increased.

2.3 Collision test results

In Table 1 the impact velocity and mass of the striker, depth of dent and header type for each test are provided. The depth-of-dent was measured at the deepest point of the plate. In Table 2 the kinetic energy of the striker, $E_k(= MV_i^2/2)$ is non-dimensionalized by $E_p(= \sigma_Y t^2\sqrt{ab})$, which may represent the energy absorption capacity of the struck plate. Consequently the energy ratio, E_k/E_p, may be a parameter to indicate the severity of the damage due to collision. The range of energy ratios of the tested models is 0.35-16.58.

The collision load histories for models A10 and C16 can be seen in Figure 3, which were obtained using a load cell installed between the header and main body of the striker. These information may be helpful to substantiate any numerical calculation results(Cho 2000). Photographs of damaged models(models B10, C28 and A23) are given in Figure 4, which showing typical damaged shapes of three different header types. In the photographs, apparent yield lines can be seen at the impinged and outer regions, but in the middle of the models plateaus were formed.

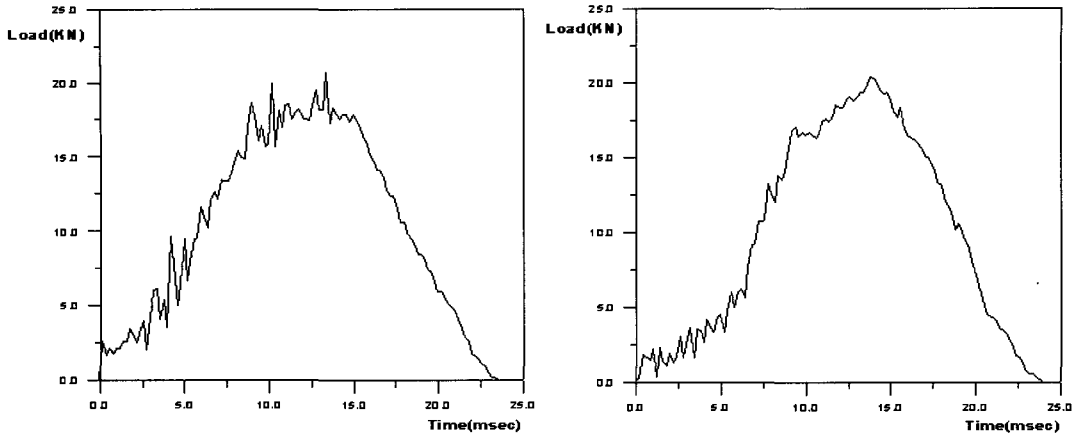

(a) model A10 (b) model C16

Figure 3: Collision load history obtained from load cell

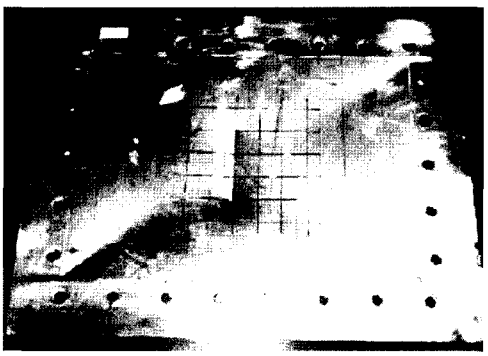

(a) model B10

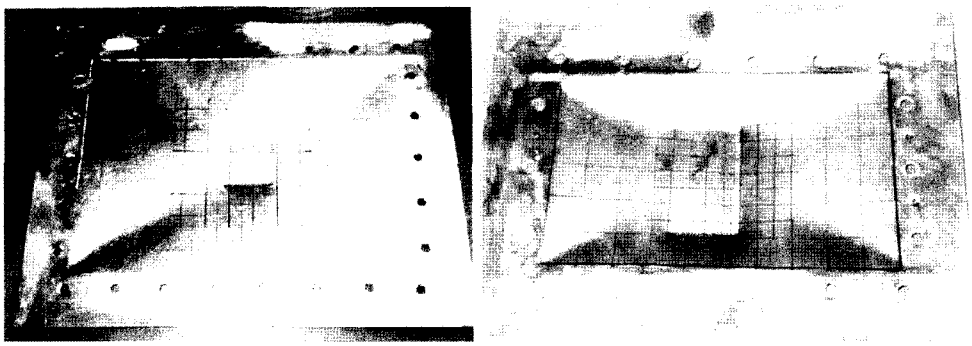

(b) model C28 (c) model A23

Figure 4: Photographs of damaged plates

Table 1: Results of plate collision tests

Model	Width×length×thick (mm)	Material properties		Striker			Depth of dent (mm)
		Yield stress (N/mm^2)	Young's Modulus (N/mm^2)	Impact Velocity (m/s)	Mass (Kg)	Header type	
A1	500×300×0.82	185	206,000	4.00	21.8	K(100)	16.50
A5	500×300×0.82	185	206,000	5.60	21.8	K(100)	21.50
A10	700×500×0.82	145	205,000	3.18	47.0	K(165)	18.65
A21	500×300×0.82	131	208,000	3.80	49.5	R	23.67
A22	500×300×0.82	131	208,000	4.78	49.5	R	25.13
A23	500×300×0.82	131	208,000	3.24	54.0	R	22.57
A27	500×300×0.82	131	208,000	4.50	49.0	S	27.27
A28	500×300×0.82	131	208,000	4.65	49.0	S	28.08
A29	500×300×0.82	131	208,000	2.63	49.0	S	17.25
A30	700×500×0.82	146	205,000	3.79	49.0	S	22.83
A31	700×500×0.82	146	205,000	5.49	49.0	S	31.90
A32	700×500×0.82	146	205,000	3.21	49.0	S	18.00
B1	500×300×1.03	161	200,000	4.15	21.8	K(100)	15.50
B2	500×300×1.03	161	200,000	5.33	21.8	K(100)	20.50
B5	500×300×1.03	161	200,000	4.15	21.8	K(100)	16.50
B6	500×300×1.03	161	200,000	5.60	21.8	K(100)	21.50
B9	500×300×1.03	140	218,000	3.74	47.0	K(165)	17.67
B10	700×500×1.03	136	222,000	3.84	51.5	K(165)	24.60
B12	700×500×1.03	136	222,000	3.56	51.5	K(165)	20.90
B21	500×300×1.03	140	218,000	2.63	60.0	K(165)	14.95
B22	500×300×1.03	140	218,000	3.47	49.5	R	21.42
B23	500×300×1.03	140	218,000	4.85	49.5	R	21.03
B24	500×300×1.03	140	218,000	3.28	49.5	R	16.00
B28	500×300×1.03	140	218,000	3.57	62.0	S	20.85
B29	500×300×1.03	140	218,000	4.34	62.0	S	33.67
B30	500×300×1.03	140	218,000	2.61	62.0	S	18.73
B31	700×500×1.03	136	222,000	3.75	49.0	S	21.82
B32	700×500×1.03	136	222,000	3.91	49.0	S	21.70
B33	700×500×1.03	136	222,000	4.70	49.0	S	30.75
C1	500×300×1.22	187	202,000	4.09	21.8	K(100)	11.50
C2	500×300×1.22	187	202,000	5.29	21.8	K(100)	18.50
C3	500×300×1.22	187	202,000	6.43	21.8	K(100)	22.50
C4	500×300×1.22	187	202,000	8.18	21.8	K(100)	32.37
C5	500×300×1.22	187	202,000	6.43	21.8	K(100)	22.50
C7	770×500×1.22	150	208,000	3.46	21.8	K(100)	12.60
C8	770×500×1.22	150	208,000	5.29	21.8	K(100)	21.30

continued on next page..

continued from previous page..

Model	Width×length×thick (mm)	Material properties		Striker			Depth of dent (mm)
		Yield stress (N/mm^2)	Young's Modulus (N/mm^2)	Impact Velocity (m/s)	Mass (Kg)	Header type	
C9	770×500×1.22	150	208,000	6.43	21.8	K(100)	26.20
C10	770×500×1.22	150	208,000	4.20	40.5	K(100)	25.90
C11	770×500×1.22	150	208,000	5.32	40.5	K(100)	34.00
C12	770×500×1.22	150	208,000	5.61	40.5	K(100)	36.18
C13	500×300×1.22	138	203,000	3.66	60.0	K(165)	20.67
C15	500×300×1.22	138	203,000	2.82	60.0	K(165)	15.80
C16	700×500×1.22	134	207,000	3.98	51.5	K(165)	21.17
C17	700×500×1.22	134	207,000	4.27	51.5	K(165)	26.60
C18	700×500×1.22	134	207,000	3.52	47.0	K(165)	19.30
C19	500×300×1.22	138	203,000	3.66	54.0	R	22.50
C20	500×300×1.22	138	203,000	2.18	54.0	R	13.55
C21	500×300×1.22	138	203,000	4.75	54.0	R	20.60
C25	500×300×1.22	138	203,000	4.04	49.0	S	20.45
C26	500×300×1.22	138	203,000	4.36	49.0	S	26.48
C27	500×300×1.22	138	203,000	3.26	49.0	S	19.83
C28	700×500×1.22	134	207,000	3.92	49.0	S	21.38
C29	700×500×1.22	134	207,000	4.06	49.0	S	26.45
C30	700×500×1.22	134	207,000	2.09	49.0	S	14.22
D1	500×300×1.60	182	206,000	3.91	21.8	K(100)	8.30
D2	500×300×1.60	182	206,000	5.63	21.8	K(100)	14.30
D3	500×300×1.60	182	206,000	6.92	21.8	K(100)	18.50
D4	500×300×1.60	182	206,000	8.18	21.8	K(100)	23.50
D5	500×300×1.60	182	206,000	6.43	21.8	K(100)	18.80
D6	500×300×1.60	182	206,000	8.11	21.8	K(100)	23.50
D7	700×500×1.61	269	214,000	5.29	21.8	K(100)	10.70
D8	700×500×1.61	269	214,000	6.92	21.8	K(100)	15.80
D9	700×500×1.61	269	214,000	7.50	21.8	K(100)	21.50
D10	700×500×1.61	269	214,000	4.39	40.5	K(100)	14.55
D11	700×500×1.61	269	214,000	5.32	40.5	K(100)	22.90
E1	700×500×2.02	286	210,000	4.74	21.8	K(100)	7.30
E2	700×500×2.02	286	210,000	6.43	21.8	K(100)	9.35
E3	700×500×2.02	286	210,000	8.18	21.8	K(100)	14.50
E4	700×500×2.02	286	210,000	5.32	40.5	K(100)	15.60

Notes: Header Type

K(100); knife(length $100mm$), K(165); knife(length $165mm$),

R: rectangular($10cm \times 17cm$), S; square($10cm \times 10cm$)

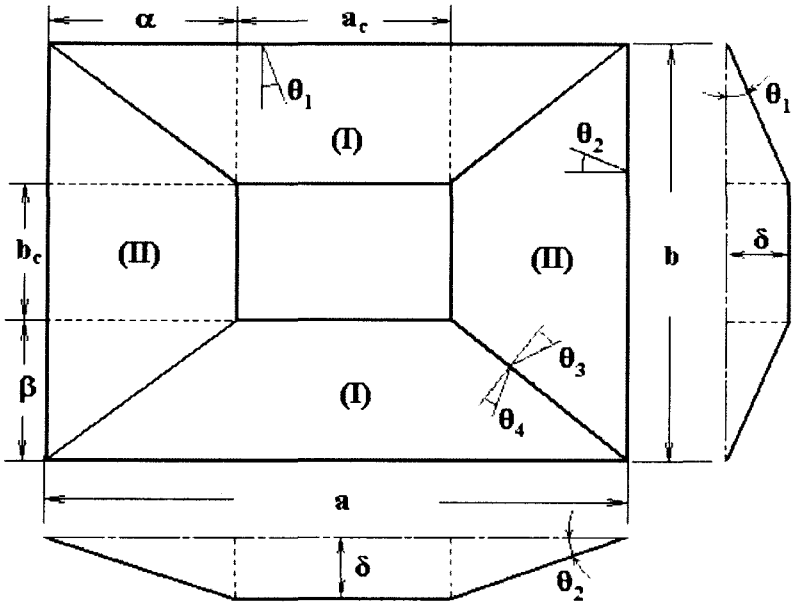

Figure 5: Assumed deformed shape of struck plate

3 Simple analytical method

A simple analytical method has been developed to predict the depth of dent of the plate due to collision. It is assumed that the kinetic energy of the striker can be dissipated by the formation of yield lines and membrane tensions of the impacted plate. The deformed shape of the damaged plate is then assumed as that shown in Figure 5. The total plastic strain energy dissipated by the impacted plate may be written as follows:

$$U_{total} = U_b + U_t = \int m_p \theta dL + \int \varepsilon_p \sigma_{YD} dV \tag{1}$$

(1) Energy dissipated by plastic bending at yield lines(U_b)

The energy dissipated by the formation of yield lines can be expressed by the rotational angle at yield lines, the length of the lines and the plastic bending moment.

$$U_b = m_p\{2(a+a_c)\theta_1 + 2(b+b_c)\theta_2 + 4l_\delta(\theta_3+\theta_4)\} \tag{2}$$

or

$$\begin{aligned} U_b = \frac{\sigma_{YD}t^2}{4}[&2(a+a_c)\tan^{-1}(\frac{\delta}{\beta}) + 2(b+b_c)\tan^{-1}(\frac{\delta}{\alpha}) \\ &+ 4l_\delta\{\tan^{-1}\frac{\beta\delta}{\sqrt{(\alpha\beta)^2+(\alpha^2+\delta^2)^2}} + \tan^{-1}\frac{\alpha\delta}{\sqrt{(\alpha\beta)^2+(\beta^2+\delta^2)}}\}] \end{aligned} \tag{3}$$

where

$$\begin{aligned} \alpha &= (a-a_c)/2 \\ \beta &= (b-b_c)/2 \\ l_\delta &= \sqrt{\alpha^2+\beta^2+\delta^2} \end{aligned}$$

(2) Energy dissipated by plastic membrane tension(U_t)

The energy dissipated by the plastic membrane tension of the plate can be divided into those of region (I) and (II) as shown in Figure 5. The plastic strain energy of each of these two regions may be written as the following expressions.

$$U_{tI} = \sigma_{YD} t(a_c + \alpha)(\sqrt{\beta^2 + \delta^2} - \beta)$$
$$U_{tII} = \sigma_{YD} t(b_c + \beta)(\sqrt{\alpha^2 + \delta^2} - \alpha)$$

Therefore the total dissipated energy by the membrane tension can be written as follows:

$$\begin{aligned} U_t &= 2(U_{tI} + U_{tII}) \\ &= 2t\{\sigma_{YDI}(a_c + \alpha)(\sqrt{\beta^2 + \delta^2} - \beta) + \sigma_{YDII}(b_c + \beta)(\sqrt{\alpha^2 + \delta^2} - \alpha)\} \end{aligned} \tag{4}$$

(3) Dynamic yield stress

The remaining task is to determine the dynamic yield stress, $\sigma_Y D$, in (3) and (4). Equation (5) is well-known and convenient equation to obtain the dynamic yield stress proposed by Cowper and Symonds(1957). For mild steel $40/sec$ and 5 can be used for Q and p in (5) respectively(Jones 1997).

$$\frac{\sigma_{YD}}{\sigma_Y} = 1 + (\frac{\dot{\varepsilon}}{Q})^{1/p} \tag{5}$$

The strain rates of regions (I) and (II) can be approximated by (6a) and (6b) respectively. Substitution of these equations into (5) provides the dynamic yield stresses of regions (I) and (II). The average of these two values is used for calculating the energy dissipated by plastic bending at yield lines given as (3).

$$\dot{\varepsilon_I} = \frac{V_i}{2} \frac{\sqrt{\alpha^2 + \delta^2} - \alpha}{\alpha\delta} \tag{6a}$$

$$\dot{\varepsilon_{II}} = \frac{V_i}{2} \frac{\sqrt{\beta^2 + \delta^2} - \beta}{\beta\delta} \tag{6b}$$

4 Discussion

The collision testing machine of spring-roller conveyer type, which was used in this study, is quite handy and easy to operate. However, the centers of impinged area were not exactly coincident with the center of the models due to the yawing motion of the striker. Modifications of the testing machine are necessary to reduce the yawing motion of the striker.

Dynamic tensile tests were performed in this study and their results are depicted in Figure 2. The dynamic yield stresses of the material used in this study were lower than those predicted by the Cowper and Symonds equation when the strain rates are larger than 0.1. The greater deviations can be seen when the strain rates become larger. It is yet premature to modify the Cowper and Symonds equation with the small number of test results.

Contrary to the results of ten dynamic tensile tests conducted(five tests each) by Campbell and Cooper(1966) and Paik et al(1999) the rupture strains were increased for greater strain rate. Therefore, further experimental investigations are necessary to quantify the strain rate effects on the material properties.

Table 2: Comparison of plate collision test results with theoretical predictions

Model	E_k/E_p	Non-dim. Depth of dent (δ/t)		Ratio (anal./exp.)	Model	E_k/E_p	Non-dim. Depth of dent (δ/t)		Ratio (anal./exp.)
		exp.	anal.				exp.	anal.	
A1	3.62	20.12	18.36	0.912	C8	2.20	17.46	16.48	0.944
A5	7.10	26.22	25.60	0.976	C9	3.25	21.48	20.02	0.932
A10	4.09	22.74	25.90	1.139	C10	2.58	21.23	17.99	0.847
A21	10.48	28.87	23.64	0.819	C11	4.14	27.87	22.74	0.816
A22	16.58	30.65	29.64	0.967	C12	4.60	29.66	23.96	0.808
A23	8.31	27.52	21.11	0.767	C13	5.05	16.94	14.81	0.874
A27	14.54	33.26	33.40	1.004	C15	3.00	12.95	11.35	0.876
A28	15.53	34.24	34.49	1.007	C16	3.46	17.35	19.13	1.102
A29	4.97	21.04	19.75	0.939	C17	3.98	21.80	20.51	0.941
A30	6.06	27.84	31.59	1.135	C18	2.47	15.82	16.15	1.021
A31	12.71	38.90	45.22	1.162	C19	4.55	18.44	12.48	0.677
A32	4.35	21.95	26.86	1.224	C20	1.61	11.11	7.33	0.660
B1	2.84	15.05	14.31	0.951	C21	7.66	16.91	16.21	0.959
B2	4.68	19.90	18.37	0.923	C25	5.03	16.76	15.87	0.947
B5	2.84	16.02	14.31	0.893	C26	5.85	21.70	17.11	0.788
B6	5.17	20.87	19.30	0.925	C27	3.27	16.25	12.81	0.788
B9	5.71	17.16	17.27	1.007	C28	3.19	17.52	18.50	1.056
B10	4.45	23.88	23.82	0.997	C29	3.42	21.68	19.16	0.884
B12	3.82	20.29	22.10	1.089	C30	0.91	11.66	9.81	0.842
B21	3.61	14.51	13.74	0.947	D1	0.92	5.19	6.16	1.187
B22	5.18	20.80	14.65	0.704	D2	1.91	8.94	9.04	1.011
B23	10.12	20.42	20.44	1.001	D3	2.89	11.56	11.17	0.966
B24	4.63	15.53	13.84	0.891	D4	4.04	14.69	13.23	0.901
B28	6.87	20.24	20.44	1.010	D5	2.50	11.75	10.37	0.883
B29	10.15	32.69	24.76	0.757	D6	3.97	14.69	13.12	0.893
B30	3.67	18.18	14.99	0.824	D7	0.74	6.65	7.90	1.189
B31	4.04	27.01	22.84	0.846	D8	1.27	9.81	10.44	1.064
B32	4.39	21.07	23.80	1.130	D9	1.49	13.35	11.33	0.848
B33	6.34	29.85	28.49	0.954	D10	0.95	9.04	9.06	1.003
C1	1.69	9.43	9.95	1.056	D11	1.39	14.22	11.05	0.777
C2	2.83	15.16	12.93	0.853	E1	0.35	3.61	4.63	1.281
C3	4.18	18.44	15.73	0.853	E2	0.65	4.63	6.45	1.393
C4	6.77	26.53	19.98	0.753	E3	1.06	7.18	8.31	1.158
C5	4.18	18.44	15.73	0.853	E4	0.83	7.72	7.39	0.957
C7	0.94	10.33	10.72	1.038					

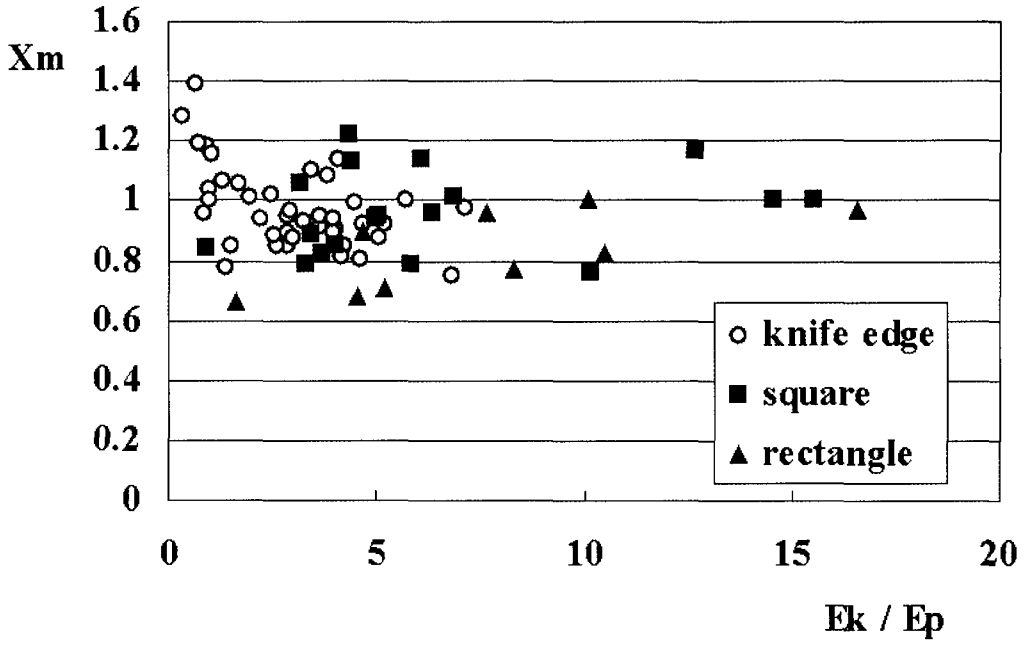

Figure 6: Skewness check of predictions by proposed analytical method

Having investigated the shape of damaged models, it is found common to all models regardless of striker header type that very apparent yield lines were formed in the outer regions. But in the middle of models, where the striker impinged, plateaus were formed rather than any apparent yield lines except those showing the shape of striker headers.

Simple analytical method has been developed in this study to predict the extent of damage on plates due to lateral collision loads. In the development, it is assumed that the kinetic energy of the striker can be dissipated by the formation of yield lines and membrane tensions in the impacted plate. The dynamic yield stress is approximated by the Cowper and Symonds equation.

The predictions of extent of damage using proposed method are given in Table 2. Comparing the predictions with test results, the ratios of predicted to experimental depth of damage, Xm, provide a mean of 0.950 together with 14.3% COV. Considering the larger uncertainties in collision tests than any static strength tests, it seems that the developed method is not only simple to use but also accurate and reliable.

As mentioned earlier when strain rate is greater than 1.0 the Cowper and Symonds equation overestimates the dynamic yield stresses by more than 10% of test results. When employ more appropriate constitutive equations the accuracy of predictions can be improved.

In the theoretical predictions the centers of impinged areas are assumed to be at the center of the models. However, for most of the tests the damaged model were not exactly symmetric. This assumption is another source of prediction uncertainty.

In Figure 6 the skewness of damage predictions are checked against energy ratio($= E_k/E_p$). It can be seen in the figure that when the energy ratio is small the scatterness becomes large. For the case of small energy ratio, elastic strain energy is comparable to that of plastic. However, for larger energy cases convergence to unity can be seen in the figure. Furthermore, no apparent distinction in prediction accuracy can be seen between the groups of different header types.

5 Conclusions

In this study, a handy collision testing machine has been designed and fabricated. Using this machine sixty-nine lateral collision tests have been successfully performed on steel plates. The test results provided in this paper are expected to be useful to substantiate any predictions by theoretical methods or design formulations.

The results of dynamic tensile tests performed as a part of experiments show that the dynamic yield stresses of the model material are less strain rate sensitive than those obtained by the Cowper and Symonds equation especially strain rate is larger than 1.0.

A simple analytical method has also been derived to predict the depth of dent of plate due to collision. In the method it is assumed that the kinetic energy of the striker can be dissipated by the formation of yield lines and membrane tensions of the impacted plate. The dynamic effects are approximately considered by using dynamic yield stresses obtained from the Cowper and Symonds constitutive equation.

Somewhat interestingly, the extent of damage predictions by the proposed analytical method provide quite good accuracy and reliability, which is not worse than any good formulations for static strength problems. It seems promising to extend this kind of approach to more complicated plated structures.

For all the tests reported in this paper neither crack nor fracture was occurred in the models. In order to apply the proposed method with confidence, further works are necessary to derive the criterion of the occurrence of crack or fracture.

References

CAMPBELL, J.D. AND COOPER, R.H. 1966 Yield and flow of low-carbon steel at medium strain rate. Proc. of the Conf. On the Physical Basis of Yield and Fracture, Institute of Physics and Physical Society, London, pp. 77-87

CHO, S.R. 2000 Numerical prediction of structural behaviours of ship's platings in side collisions. J. of Engineering Research, **31**, **2**, pp. 133-144

COWPER, G.R. AND SYMONDS, P.S. 1957 Strain-Hardening and strain-rate effects in the impact loading of cantilever beams. Tech. Rep. Brown Univ, **28**

FRIEZE, P.A. AND CHO. S.R. 1989 Dynamic impact to tubulars and their residual strength. Proc. 4th Int'l Symp. on Practical Design of Ship and Mobile Units(PRADS '89), Varna, pp. 50/1-50/7

JONES, N. 1997 Structural impact. Cambridge University Press, Cambridge, pp. 348-355

KITAMURA, O. AND KUROIWA, T. 1996 Large-scale grounding experiments and numerical simulations. Ship Technology Research, **34**, **4**, pp. 62-69

PAIK, J.K. ET AL 1999 On rational design of double hull taker structure against collision. The 1999 annual meeting of the Society of Naval Architects and Marine Engineers.

SAMUELIDES, E. 1984 Structural dynamic and rigid body response coupling in ship collision. PhD Thesis, Glasgow Univ.

ZHU, L. AND FAULKNER, D. 1993 Dynamic inelastic behaviour of plates in minor ship collisions. Int'l J. of Impact Engineering, **15**, **2**, pp. 165-178